Buckling of Thin Cylinder under Combined External Pressure and Axial Compression

G. Krishnamoorthy*
California State University, San Diego, Calif.

In this paper a deflection function with undetermined coefficients is used to determine analytically the bifurcation buckling load of a cylindrical tube under combined external pressure and axial compression using Donnell's simplified equations. This procedure can be adopted for various types of prescribed boundary conditions. In order to demonstrate the feasibility of this method, only the fixed-end conditions are considered for solution in this paper. The results obtained for the fixed-end conditions indicate that the critical buckling value depends on the ratio of thickness to radius and not on the ratio of radius to length and the critical buckling value decreases as the ratio of circumferential compressive stress to axial compressive stress increases. The buckling interaction curve for combined radial and axial compression for this case appears to follow a straight line indicating a uniform percentage decrease in the axial compressive load from the theoretical classical value for uniform axial compression.

Nomenclature

A_1 to A_4	= arbitrary constants
a_1 to a_8	
$b_1, b_2 \bar{b}_1, \bar{b}_2$	
$c_1, c_2, \bar{c}_1, \bar{c}_2$	= see Eq. (19)
$C_{ij=i,j}$	= 1 to 4 matrix and determinant elements
D	= see Eq. (2)
E	= modulus of elasticity
e_1, e_2	= see Eq. (23)
K	= see Eq. (6)
K_x, K_y	= see Eq. (2)
L	= length of the shell
m	= see Eq. (2)
n	= mode number = 1,2,3, ...
p	= see Eq. (10)
$\bar{p}_1$ to $\bar{p}_6$	= see Eq. (20)
p_1 to p_6	
R	= radius of the middle surface of the shell
t	= thickness of the shell
u,v,w	= displacement in the x,y,z directions respectively
x,y,z	= right-handed coordinate system
Z	= see Eq. (6)
α	= $n/2\pi R$ see Eq. (3)
λ_1, β_1	= real and imaginary part of Eq. (8) respectively
λ_2, β_2	= real and imaginary part of Eq. (9) respectively
μ	= Poisson's ratio
η	= see Eq. (6)
σ_{cl}	= buckling strength of moderate length of cylinder, see Eq. (7)
σ_x	= normal compressive stress in the axial x direction
σ_y	= transverse compressive stress in the circumferential y direction
Φ_1 to Φ_4	= see Eqs. (8) and (9)
φ_1 to φ_4	= indicial roots, see Eqs. (8) and (9)

THERE is a vast amount of literature on the buckling of thin shells and a review up to 1958 can be found in an article by Y. C. Fung and E. E. Sechler.[1] A summary of available solutions can be found in the Handbook of Engineering Mechanics[2] and the Handbook for Structural Stability.[3,4] Most of the literature involves calculation of the buckling strength of a cylindrical tube by assuming suitable deflection functions that will satisfy the boundary conditions.

Received November 3, 1972; revision received September 4, 1973.
Index category: Structural Stability Analysis.
*Associate Professor of Civil Engineering.

It is difficult to apply these methods for thin shells with various edge conditions. In this paper a general deflection function with undetermined coefficients is assumed, which can be made to satisfy any prescribed boundary conditions. This type of function gives an exact solution of the governing differential equations. In order to demonstrate the feasibility of such a method, the buckling of a closed cylinder with fixed ends subjected simultaneously to uniform radial and uniform axial force is illustrated in this paper.

The simplified equations of the small deflection theory known as Donnell's equations[5] are used. Although the small deflection theory may give buckling stresses higher than the actual buckling values, it will serve the purpose of establishing upper bounds of the buckling loads.

Coordinates and Displacements

The dimensions of the cylindrical shell are given by the length L, thickness t, and radius R to the middle surface. The origin of a right-handed coordinate system x, y, z, is at the midlength of the middle surface of the shell. The coordinate x is parallel to the axis of the cylinder. The coordinate y is in the circumferential direction. The coordinate z is in the radial direction and is positive outward. The displacements in the positive directions of x, y, and z are referred to as u, v, and w, respectively.

General Equations

Donnell's equations for a cylindrical tube subjected to an axial compressive stress σ_x and a circumferential compressive stress σ_y can be written as

$$\nabla^8 w + \frac{12m^2}{L^4}\frac{\partial^4 w}{\partial x^4} + \frac{\pi^2}{L^2}\nabla^4 \left[K_x \frac{\partial^2 w}{\partial x^2} + K_y \frac{\partial^2 w}{\partial y^2} \right] = 0 \quad (1)$$

where

$$K_x = \frac{\sigma_x t L^2}{\pi^2 D}; \; K_y = \frac{\sigma_y t L^2}{\pi^2 D};$$
$$m = \frac{L^2}{Rt}(1-\mu^2)^{1/2}; \; D = \frac{Et^3}{12(1-\mu^2)} \quad (2)$$

Solution for Critical Stress

The general solution of w obtained from Eq. (1) will have eight arbitrary constants. From this solution, the displacements of u, v, w, and all the stress resultants can be easily obtained using the uncoupled Donnell's equations. These expressions so derived with eight undetermined coefficients must satisfy the prescribed fixed-end boundary conditions. The boundary conditions are satisfied by setting the expressions, u, v, w and $\partial w/\partial x$ equal to zero at both ends of the cylinder, i.e., at $x = L/2$ and $x = -L/2$. The critical buckling stress is then obtained by setting the determinant of the boundary expressions, which are functions of the arbitrary constants, equal to zero.

General Solution for w

In order to obtain a general solution to satisfy Eq. (1), the following expression for w is assumed

$$w = \{ae^{\Phi x}\}\cos\alpha y \text{ where } \alpha = \frac{n}{2\pi R} \text{ and } \Phi \text{ is constant.} \quad (3)$$

Substituting Eq. (3) into Eq. (1), the following indicial equation is obtained

$$\Phi^8 + \left(\frac{K_x\pi^2}{\alpha^2L^2} - 4\right)\Phi^6\alpha^2 + \left(6 + \frac{12m^2}{\alpha^4L^4} - \frac{2K_x\pi^2}{\alpha^2L^2} - \frac{K_y\pi^2}{\alpha^2L^2}\right)\Phi^4\alpha^4 + \left(\frac{2K_x\pi^2}{\alpha^2L^2} + \frac{K_y\pi^2}{\alpha^2L^2} - 4\right)\Phi^2\alpha^6 + \left(-\frac{K_y\pi^2}{\alpha^2L^2} + 1\right)\alpha^8 = 0 \quad (4)$$

A direct numerical solution of Eq. (4) biquadratic in Φ^2 is impossible even with a precision of sixteen digits because of the numerical sensitivity of extremely small differences of very large numbers. Therefore, Eq. (4) is rewritten in the following quadratic form in $[(\Phi^2 - 1)^2/\Phi^2]$:

$$\left[\frac{(\phi^2-1)^2}{\phi^2}\right]^2 + K\left[\frac{(\phi^2-1)^2}{\phi^2}\right] + Z = 0 \quad (5)$$

$$\phi = \frac{\Phi}{\alpha}\,;\; K = \frac{K_x\pi^2}{\alpha^2L^2}\left(1 - \frac{\eta}{\phi^2}\right);\; \eta = \frac{K_y}{K_x}\,;\; Z = \frac{12m^2}{\alpha^4L^4} \quad (6)$$

It is found that the roots can be evaluated for the entire implicit quadratic expression as shown in Eq. (5). Then the actual roots of ϕ are obtained by solving the roots of the implicit quadratic expression in ϕ. As a first approximation the roots are obtained assuming η to be zero, in which case the term involving η/ϕ^2 will vanish. For the second and subsequent approximations, the roots obtained in the previous approximation is used with the proper value of η. This iteration process is continued until the desired degree of accuracy is achieved. Usually three iterative evaluations are enough to obtain a reasonable degree of accuracy.

The cylindrical shell subjected to axial as well as radial pressure having a critical buckling stress less than or equal to the classical buckling stress

$$\sigma_{c1} = \frac{1}{(3)^{1/2}(1-\mu^2)^{1/2}}\frac{Et}{R} \quad (7)$$

is of primary interest in this study. Therefore, the roots of Eq. (5) are written in the form

$$\left.\begin{matrix}\pm\Phi_1 = \pm\phi_1\alpha \\ \pm\Phi_2 = \pm\phi_2\alpha\end{matrix}\right\} = \pm(\gamma_1 \pm i\beta_1)\alpha = \pm[1-(p+iq)^{1/2} \pm i(p+iq)^{1/2}]\alpha \quad (8)$$

$$\left.\begin{matrix}\pm\Phi_3 = \pm\phi_3\alpha \\ \pm\Phi_4 = \pm\phi_4\alpha\end{matrix}\right\} = \pm(\gamma_2 \pm i\beta_2)\alpha = \pm[1-(p-iq)^{1/2} \pm i(p-iq)^{1/2}]\alpha \quad (9)$$

where

$$p = \frac{Z^{1/2}}{4}\left(\frac{K}{2Z^{1/2}}\right) = \frac{Z^{1/2}}{4}\frac{\sigma_x}{\sigma_{cl}}\left(1 - \frac{\eta}{\phi^2}\right) \quad (10)$$

$$q = \frac{Z^{1/2}}{4}\left[1 - \left(\frac{K}{2Z^{1/2}}\right)^2\right]^{1/2} = \frac{Z^{1/2}}{4}\left[1 - \left(\frac{\sigma_x}{\sigma_{cl}}\right)^2\left(1 - \frac{\eta}{\phi^2}\right)\right]^{1/2} \quad (11)$$

From the above equations it may be seen that the eight roots of the indicial equation form four sets of complex conjugates, yielding the following solution for w:

$$\begin{aligned} w = [\, & e^{\alpha\gamma_1 x}(a_1 \sin\alpha\beta_1 x + a_2 \cos\alpha\beta_1 x) \\ & + e^{\alpha\gamma_2 x}(a_3 \sin\alpha\beta_2 x + a_4 \cos\alpha\beta_2 x) \\ & + e^{-\alpha\gamma_1 x}(a_5 \sin\alpha\beta_1 x + a_6 \cos\alpha\beta_1 x) \\ & + e^{-\alpha\gamma_2 x}(a_7 \sin\alpha\beta_2 x + a_8 \cos\alpha\beta_2 x)]\cos\alpha y \end{aligned} \quad (12)$$

The expressions for u and v can be obtained from Eq. (12) using the uncoupled Donnell's equations.

A shell with symmetrical boundary conditions and loadings may buckle either into a symmetrical or into an antisymmetrical deflection pattern. Hence, it will be convenient to separate the symmetrical and antisymmetrical parts for w, u, v, and $\partial w/\partial x$. In order to satisfy the symmetrical and antisymmetrical deflection conditions along the axial direction the coefficients must satisfy the following relationships respectively:

$$a_5 = -a_1\,;\; a_6 = a_2\,;\; a_7 = -a_3\,;\; a_8 = a_4 \quad (13)$$

$$a_5 = a_1\,;\; a_6 = -a_2\,;\; a_7 = a_5\,;\; a_8 = -a_4 \quad (14)$$

Using the above relationship, the symmetrical and the antisymmetrical solutions for w, u, v, and $\partial w/\partial x$ are written with a set of four new constants, A_1, A_2, A_3, and A_4.

Equations for w, u, v, and ∂w/∂x

With the subscript S referring to the symmetric part and the subscript A referring to the antisymmetric part, the final equations are

$$\left.\begin{matrix} w_S \\ w_A \end{matrix}\right\} = \Big[A_1 \genfrac{}{}{0pt}{}{\cosh\alpha\gamma_1 x}{\sinh\alpha\gamma_1 x}\cos\alpha\beta_1 x + A_2\genfrac{}{}{0pt}{}{\sinh\alpha\gamma_1 x}{\cosh\alpha\gamma_1 x}\sin\alpha\beta_1 x + A_3\genfrac{}{}{0pt}{}{\cosh\alpha\gamma_2 x}{\sinh\alpha\gamma_2 x}\cos\alpha\beta_2 x + A_4\genfrac{}{}{0pt}{}{\sinh\alpha\gamma_2 x}{\cosh\alpha\gamma_2 x}\sin\alpha\beta_2 x\Big]\cos\alpha y \quad (15)$$

$$\begin{aligned} \left.\begin{matrix} u_S \\ u_A \end{matrix}\right\} = \Big\{ & A_1\Big[\genfrac{}{}{0pt}{}{\sinh\alpha\gamma_1 x}{\cosh\alpha\gamma_1 x}\, b_1\cos\alpha\beta_1 x + \genfrac{}{}{0pt}{}{\cosh\alpha\gamma_1 x}{\sinh\alpha\gamma_1 x}\, b_2\sin\alpha\beta_1 x\Big] \\ & + A_2\Big[\genfrac{}{}{0pt}{}{\sinh\alpha\gamma_1 x}{\cosh\alpha\gamma_1 x}(-b_2)\cos\alpha\beta_1 x + \genfrac{}{}{0pt}{}{\cosh\alpha\gamma_1 x}{\sinh\alpha\gamma_1 x}\, b_1\sin\alpha\beta_1 x\Big] \\ & + A_3\Big[\genfrac{}{}{0pt}{}{\sinh\alpha\gamma_2 x}{\cosh\alpha\gamma_2 x}\, \bar{b}_1\cos\alpha\beta_2 x + \genfrac{}{}{0pt}{}{\cosh\alpha\gamma_2 x}{\sinh\alpha\gamma_2 x}\, \bar{b}_2\sin\alpha\beta_2 x\Big] \\ & + A_4\Big[\genfrac{}{}{0pt}{}{\sinh\alpha\gamma_2 x}{\cosh\alpha\gamma_2 x}(-\bar{b}_2)\cos\alpha\beta_2 x + \genfrac{}{}{0pt}{}{\cosh\alpha\gamma_2 x}{\sinh\alpha\gamma_2 x}\, \bar{b}_1\sin\alpha\beta_2 x\Big]\Big\}\cos\alpha y \end{aligned} \quad (16)$$

$$\begin{aligned} \left.\begin{matrix} v_S \\ v_A \end{matrix}\right\} = \Big\{ & A_1\Big[\genfrac{}{}{0pt}{}{\cosh\alpha\gamma_1 x}{\sinh\alpha\gamma_1 x}\, c_1\cos\alpha\beta_1 x + \genfrac{}{}{0pt}{}{\sinh\alpha\gamma_1 x}{\cosh\alpha\gamma_1 x}\, c_2\sin\alpha\beta_1 x\Big] \\ & + A_2\Big[\genfrac{}{}{0pt}{}{\cosh\alpha\gamma_1 x}{\sinh\alpha\gamma_1 x}(-c_2)\cos\alpha\beta_1 x + \genfrac{}{}{0pt}{}{\sinh\alpha\gamma_1 x}{\cosh\alpha\gamma_1 x}\, c_1\sin\alpha\beta_1 x\Big] \\ & + A_3\Big[\genfrac{}{}{0pt}{}{\cosh\alpha\gamma_2 x}{\sinh\alpha\gamma_2 x}\, \bar{c}_1\cos\alpha\beta_2 x + \genfrac{}{}{0pt}{}{\sinh\alpha\gamma_2 x}{\cosh\alpha\gamma_2 x}\, \bar{c}_2\sin\alpha\beta_2 x\Big] \\ & + A_4\Big[\genfrac{}{}{0pt}{}{\cosh\alpha\gamma_2 x}{\sinh\alpha\gamma_2 x}(-\bar{c}_2)\cos\alpha\beta_2 x + \genfrac{}{}{0pt}{}{\sinh\alpha\gamma_2 x}{\cosh\alpha\gamma_2 x}\, \bar{c}_1\sin\alpha\beta_2 x\Big]\Big\}\sin\alpha y \end{aligned} \quad (17)$$

$$\begin{aligned} \left.\begin{matrix} \left(\frac{\partial w}{\partial x}\right)_S \\ \left(\frac{\partial w}{\partial x}\right)_A \end{matrix}\right\} = \Big\{ & A_1\Big[\genfrac{}{}{0pt}{}{\sinh\alpha\gamma_1 x}{\cosh\alpha\gamma_1 x}\, \gamma_1\cos\alpha\beta_1 x + \genfrac{}{}{0pt}{}{\cosh\alpha\gamma_1 x}{\sinh\alpha\gamma_1 x}(-\beta_1)\sin\alpha\beta_1 x\Big] \\ & + A_2\Big[\genfrac{}{}{0pt}{}{\sinh\alpha\gamma_1 x}{\cosh\alpha\gamma_1 x}\, \beta_1\cos\alpha\beta_1 x + \genfrac{}{}{0pt}{}{\cosh\alpha\gamma_1 x}{\sinh\alpha\gamma_1 x}\, \gamma_1\sin\alpha\beta_1 x\Big] \\ & + A_3\Big[\genfrac{}{}{0pt}{}{\sinh\alpha\gamma_2 x}{\cosh\alpha\gamma_2 x}\, \gamma_2\cos\alpha\beta_2 x + \genfrac{}{}{0pt}{}{\cosh\alpha\gamma_2 x}{\sinh\alpha\gamma_2 x}(-\beta_2)\sin\alpha\beta_2 x\Big] \\ & + A_4\Big[\genfrac{}{}{0pt}{}{\sinh\alpha\gamma_2 x}{\cosh\alpha\gamma_2 x}\, \beta_2\cos\alpha\beta_2 x + \genfrac{}{}{0pt}{}{\cosh\alpha\gamma_2 x}{\sinh\alpha\gamma_2 x}\, \gamma_2\sin\alpha\beta_2 x\Big]\Big\}\sin\alpha y \end{aligned} \quad (18)$$

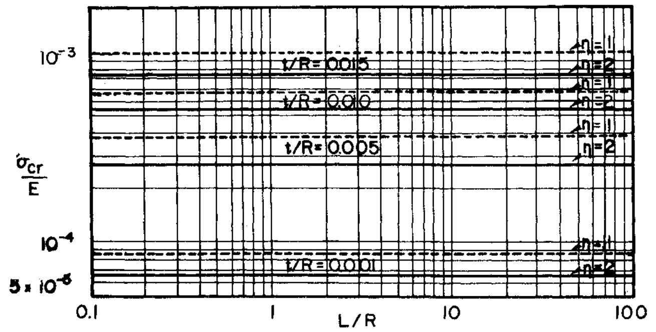

Fig. 1 Curves of σ_{cr}/E vs L/R.

where

$$b_1 = -\frac{(P_1P_3 + P_2P_4)}{(n/2\pi)(P_1^2 + P_2^2)} \; ; \quad \bar{b}_1 = -\frac{(\bar{P}_1\bar{P}_3 + \bar{P}_2\bar{P}_4)}{(n/2\pi)(\bar{P}_1^2 + \bar{P}_2^2)}$$

$$b_2 = \frac{(-P_1P_4 + P_2P_3)}{(n/2\pi)(P_1^2 + P_2^2)} \; ; \quad \bar{b}_2 = \frac{(-\bar{P}_1\bar{P}_4 + \bar{P}_2\bar{P}_3)}{(n/2\pi)(\bar{P}_1^2 + \bar{P}_2^2)} \tag{19}$$

$$c_1 = -\frac{(P_1P_5 + P_2P_6)}{(n/2\pi)(P_1^2 + P_2^2)} \; ; \quad \bar{c}_2 = -\frac{(\bar{P}_1\bar{P}_5 + \bar{P}_2\bar{P}_6)}{(n/2\pi)(\bar{P}_1^2 + \bar{P}_2^2)}$$

$$c_2 = \frac{(-P_1P_6 + P_2P_5)}{(n/2\pi)(P_1^2 + P_2^2)} \; ; \quad \bar{c}_2 = \frac{(-\bar{P}_1\bar{P}_6 + \bar{P}_2\bar{P}_5)}{(n/2\pi)(\bar{P}_1^2 + \bar{P}_2^2)}$$

$$P_1 = \gamma_1^4 - 6\gamma_1^2\beta_1^2 + \beta_1^4 - 2\gamma_1^2 + 2\beta_1^2 + 1$$

$$\bar{P}_1 = \gamma_2^4 - 6\gamma_2^2\beta_2^2 + \beta_2^4 - 2\gamma_2^2 + 2\beta_2^2 + 1$$

$$\begin{aligned} P_2 &= 4\beta_1^3\gamma_1 - 4\gamma_1^3\beta_1 + 4\gamma_1\beta_1 \; ; & \bar{P}_2 &= 4\beta_2^3\gamma_2 - 4\gamma_2^3\beta_2 + 4\gamma_2\beta_2 \\ P_3 &= \mu(\gamma_1^3 - 3\beta_1^2\gamma_1) + \gamma_1 \; ; & \bar{P}_3 &= \mu(\gamma_2^3 - 3\beta_2^2\gamma_2) + \gamma_2 \\ P_4 &= \mu(\beta_1^3 - 3\beta_1\gamma_1^2) - \beta_1 \; ; & \bar{P}_4 &= \mu(\beta_2^3 - 3\beta_2\gamma_2^2) - \beta_2 \\ P_5 &= -(2 + \mu)(\gamma_1^2 - \beta_1^2) + 1 \; ; & \bar{P}_5 &= -(2 + \mu)(\gamma_2^2 - \beta_2^2) + 1 \\ P_6 &= (2 + \mu)(2\gamma_1\beta_1) \; ; & \bar{P}_6 &= (2 + \mu)(2\gamma_2\beta_2) \end{aligned} \tag{20}$$

Determination of Buckling Stress

For either symmetrical or antisymmetrical buckling, the following boundary conditions must be satisfied along the fixed ends

$$w = 0,\; u = 0,\; v = 0 \text{ and } \partial w/\partial x = 0; \text{ at } x = + L/2 \tag{21}$$

For $x = +L/2$, Eqs. (15-18) can be written in a 4 × 4 matrix form for either symmetric or antisymmetric modes of buckling factoring common terms as shown in the following Eq. (22). The factoring out of the terms e_1 in the first two rows and e_2 in the last two rows reduces the magnitude of the elements of the matrix for convenient evaluation of the value of the determinant

$$\begin{bmatrix} w \\ u \\ v \\ \partial w/\partial x \end{bmatrix} = \begin{bmatrix} C_{1,1} & C_{1,2} & C_{1,3} & C_{1,4} \\ C_{2,1} & C_{2,2} & C_{2,3} & C_{2,4} \\ C_{3,1} & C_{3,2} & C_{3,3} & C_{3,4} \\ C_{4,1} & C_{4,2} & C_{4,3} & C_{4,4} \end{bmatrix} \times \begin{bmatrix} A_1e_1 \\ A_2e_1 \\ A_3e_2 \\ A_4e_2 \end{bmatrix} = \begin{bmatrix} 0 \\ 0 \\ 0 \\ 0 \end{bmatrix} \tag{22}$$

where

$$e_1 = {}_{1/2}e^{(\alpha\gamma_1 L/2)} \; ; \; e_2 = {}_{1/2}e^{(\alpha\gamma_2 L/2)} \tag{23}$$

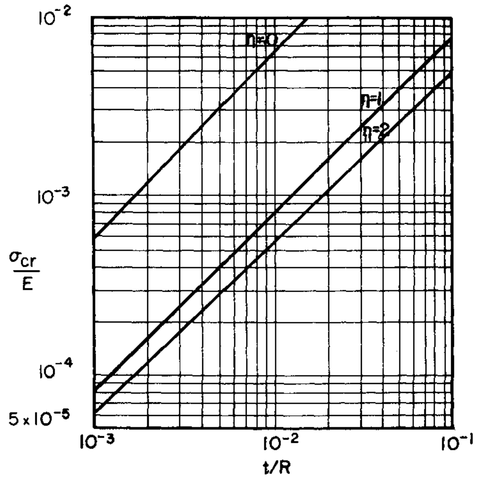

Fig. 2 Curves of σ_{cr}/E vs t/R.

The critical compressive stress value, σ_{cr} will be found by setting the determinant of the matrix $[C]$ of Eq. (22) to zero, i.e.,

$$|C| = 0 \tag{24}$$

Limiting Value of the Buckling Stress

It may be shown that the upper limit of buckling stress of a cylindrical tube, subjected to axial compressive stress alone is σ_{c1}, as given in Eq. (7). This satisfies Eq. (22) for either the symmetrical or the antisymmetrical buckling case. When $\sigma_x = \sigma_{c1}$ and $\eta = 0$, the discriminant of Eq. (5) vanishes, yielding two sets of identical roots. For this special case it can be easily verified from Eqs. (8) and (9) that $\Phi_1 = \Phi_3$ and $\Phi_2 = \Phi_4$. Hence the elements of columns 1 and 2 are identically equal to those in columns 3 and 4, respectively, in matrix $[C]$ of Eq. (22) which makes the determinant of the matrix to vanish. This verifies the fact that σ_{c1} is the limiting value of buckling stress for $\eta = 0$.

Computer Solution of Buckling Stress

The compressive stress is implicitly involved in all the matrix elements. The critical stress is therefore obtained by numerical methods using an electronic digital computer, as direct algebraic calculations is impossible. Starting from the value zero, the stress is progressively increased in small increments until the sign of the value of the determinant changes. The change in sign indicates the presence of a buckling value between the previous value and the present value of stress. The interval of search is then narrowed until the desired degree of accuracy is obtained. Thus the critical buckling stress is obtained for a given value of t/R, L/R, η for various values of n for symmetric as well as antisymmetric cases.

Conclusions

The nondimensional critical axial strain values σ_{cr}/E vs L/R ratios for $\eta = 1$ and $\eta = 2$ are plotted in Fig. 1 for values of t/R = 1/1,000, 5/1,000, 10/1,000, and 15/1,000 for a Poisson's ratio $\mu = 0.3$. It may be seen from this figure that the critical buckling stress of a cylindrical tube with clamped ends subjected to combined axial and circumferential compressive stress depends only on the ratio of thickness to radius and not on the ratio of length to radius. In Fig. 2 critical axial stress values σ_{cr}/E vs t/R ratios for values of η = 0, 1, and 2 are plotted. From this figure it may be concluded that the critical axial buckling stress of a cylindrical tube subjected to combined axial and radial pressure is about one-sixth of the axial buckling value of a corresponding cylindrical tube. As the ratio of circumferential compressive stress to axial compressive stress increases, as expected, the critical axial buckling stress value decreases. It is also found that the critical buckling stress for combined axial and radial compressive cases investigated here is independent of n.

The nondimensional critical axial strain values of σ_{cr}/E vs t/R ratios for $\eta = 0$, $\eta = 1$, and $\eta = 2$ are plotted in Fig. 2. The buckling interaction curves for combined circumferential and axial compression for clamped cylinders (i.e., for $\eta = 1$ and $\eta = 2$) appear to follow almost a straight line parallel to theoretical classical values for uniform axial compression (i.e., for $\eta = 0$), indicating a uniform percentage decrease in the axial compressive load. The experimental results of V. I. Weingarten and P. Seide[6] for cylinders with simply supported edge conditions indicated the same phenomena observed in this study for clamped cylinders, that the interaction curve between external pressure and axial compression depends on the ratio of thickness to radius.

References

[1]Fung, Y. C. and Sechler, E. E., "Instability of Thin Elastic Shells," *Structural Mechanics, Proceedings of the First Symposium on Naval Structural Mechanics,* Pergamon Press, 1960.

[2]Flügge, W., *Handbook of Engineering Mechanics,* McGraw-Hill, New York, 1962.

[3]Gerard, G. and Becker, H., "Handbook of Structural Stability Part III, Buckling of Curved Plates and Shells," TN D-163, 1959, NACA.

[4]Gerard, G., "Handbook of Structural Stability Part III, Buckling of Curved Plates and Shells," TN D-163, 1959, NACA.

[5]Donnell, L. H., "Stability of Thin Walled Tubes Under Torsion," Rept. 479, 1933, NACA.

[6]Weingarten, V. I. and Seide, P., "Elastic Stability of Thin Walled Cylindrical and Conical Shells Under Combined External Pressure and Axial Compression," *Journal of American Institute of Aeronautics and Astronautics,* Vol. 3, No. 5, May 1965.

FEBRUARY 1974 J. AIRCRAFT VOL. 11, NO. 2

Advanced Beaded and Tubular Structural Panels

Max D. Musgrove* and Bruce E. Greene†
Boeing Aerospace Company, Seattle, Wash.
and
John L. Shideler‡ and Herman L. Bohon§
NASA-Langley Research Center, Hampton, Va.

A review is presented of an NASA program to develop lightweight beaded and tubular structural panels which can be applied where beaded external surfaces are acceptable acerodynamically or where primary structure is protected by heat shields. The design shapes were obtained with an optimization computer code which interates geometric parameters to satisfy strength, stability and weight constraints. Methods of fabricating these new configurations are discussed. Nondestructive testing produced extensive combined compression, shear and bending test data on local buckling specimens and large panels. The optimized design concepts offer 25 to 40% weight savings compared to conventional stiffened sheet construction.

I. Introduction

FOR several years Langley Research Center and other NASA agencies have been investigating structural concepts which use elements with curved cross sections to develop beaded or corrugated skin panel structure.[1-5] The curved sections exhibit high local buckling strength which leads to highly efficient structural concepts. These concepts can be applied where a lightly beaded external surface is aerodynamically acceptable or where the primary structure is protected by heat shields. Their corrugated nature makes them especially attractive for high temperature application because the controlled thermal growth minimizes thermal stress. The technology resulting from this program is applicable to many areas such as launch vehicles, space shuttle, and hypersonic aircraft.

A contractual study (NAS1-10749) is in progress by The Boeing Company to develop lightweight structural panels designed for combined loads of inplane compression, inplane shear and bending due to lateral pressure. Under this contract, governing analytical static strength equations for panels under combined load, and material and geometric constraint equations were incorporated in a random search type optimization computer program[6] to identify minimum weight designs for several potentially efficient concepts. However, if these concepts are to realize their analytical potential, all failure modes must be properly recognized and accounted for. Consequently, buckling tests were conducted on subpanels to identify local failure modes and provide for proper modification of local buckling theory. Also, full scale panels (40 × 40 in.) were tested under combined loading to obtain large panel failure data for correlation with theory. A nondestructive force-stiffness test technique[7] was used to provide exten-

Presented as Paper 73-370 at the AIAA/ASME/SAE 14th Structures, Structural Dynamics, and Materials Conference, Williamsburg, Virginia, March 20–22, 1973; submitted April 26, 1973; revision received December 18, 1973. The authors wish to express their thanks to G. A. Jensen for preparing the drafts of this paper.

Index categories: Aircraft Structural Design (Including Loads); Structural Design, Optimal; Structural Static Analysis.

*Senior Specialist Engineer, Structural Allowables and Military Structures, Research and Engineering Division. AIAA Member.

†Senior Specialist Engineer, Structural Allowables and Military Structures, Research and Engineering Division.

‡ Aerospace Engineer, Thermal Section, Structures and Dynamics Division.

§ Head, Thermal Structures Section, Structures and Dynamics Division. AIAA Member.